Image Analysis of Liquid Breakup in a Low Pressure Flat Fan Spray for the Development of a Fully-Lagrangian Modelling Approach

Zuhaib Nissar, Steven Begg, Oyuna Rybdylova*
Advanced Engineering Centre, School of Architecture, Technology and Engineering, University of Brighton, Brighton, BN2 4GJ, UK
*Corresponding author: o.rybdylova@brighton.ac.uk

Abstract
The current work is focused on the development of a suitable methodology to determine droplet distribution data in a planar, flat fan spray atomisation process. The aim is to support the development of a new simulation framework, based upon the fully Lagrangian approach (FLA), that has been generalised to polydisperse evaporating droplets (gFLA). The FLA has advantages of both Lagrangian droplet tracking and continuous formulations for the admixture. Validation of this modelling approach requires the identification of transient droplet size distributions, unlike more routinely used techniques, that measure size distributions at a single point location, over the entire period.

Keywords
Atomisation, droplet distribution, optical diagnostics, image analysis.

Introduction
Sprays are commonly used in various engineering technologies [1], including fuel injection in internal combustion engines [2]. While modelling of sprays is well developed, it has been identified that the fully Lagrangian approach (FLA) has potential to accelerate the calculations, while capturing the complex structures in flow related to droplet accumulation and droplet trajectory crossing [3, 4]. In the recent paper [5], the FLA was generalised and applied to polydisperse evaporating droplets. Therefore there is a need to validate the new approach against experimental data. This requires development of the experimental techniques to capture instantaneous droplet distributions in space and size.
The present study is based on a flat fan spray in order to develop a methodology for 2D droplet distribution reconstruction. The analysis is based on image processing in order to provide a description of the liquid break up by identification of liquid structures in the spray.
The paper is arranged as follows: Section 1 is dedicated to the description of the experimental setup; the details of the image processing algorithms are presented in Section 2; the results are discussed in Section 3; and the findings are summarised in Conclusions (Section 4).

Experimental setup
The spray system consists of a commercial flat fan nozzle to inject low pressure water under steady flow conditions via a Bosch pressure washer pump under atmospheric conditions. The flat fan nozzle (BETE - BJH 0.28) is a slit type of nozzle, with a slit angle of 50 degrees and width of 0.28 mm. It is designed to produce a diverging flat spray sheet. The atomisation is assumed to occur such that the liquid sheet breaks up into droplets that are contained within the 2D spray plane, with minimal out of plane deviation.
A Photron SA4 Fastcam, a K2 Infinity long-distance microscope and a CF-1 objective lens were used to capture images with a resolution of 20 μm/pixel and a field of view of 16 $\times$ 20.48 mm^2. The high-speed camera position was perpendicular to the spray plane. Back illumination, using a pulsating LED (Cree XLamp XT-E Royal Blue) with a pulse duration of 10 μs was run synchronously with the camera. The light source was diffused to obtain a homogeneous illumination over the wider region of interest. In back illumination (shadowgraphy), the intensity

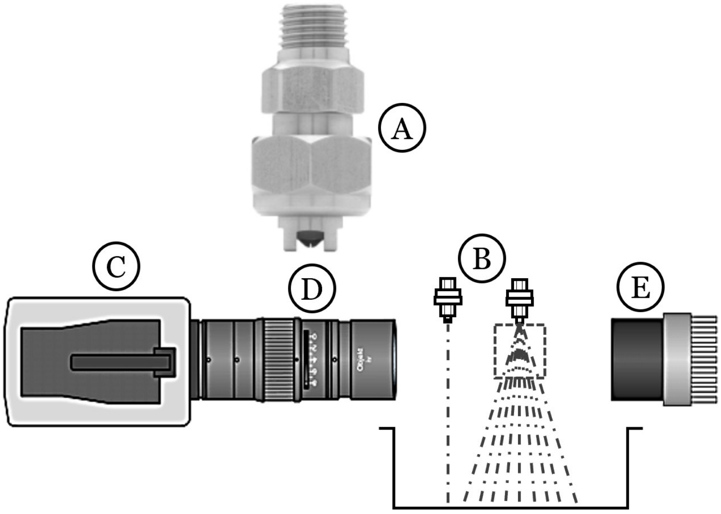

Figure 1. Diagram of the experimental setup; A Flat fan nozzle, B Flat fan spray, C Camera Photron SA4 Fastcam, D Long-distance microscopic lens.

values in the image correspond to the second spatial derivative of the refractive index. Consecutive images were recorded at a frame rate of 5000 Hz with liquid pressure of 10 bar. The optical setup is shown in Fig. 1.

Image processing algorithm

The purpose of the image processing is identification of the structures in the spray in order to conduct the analysis of the liquid break up. The following steps were undertaken in our image processing algorithm. A raw image from the camera was in a grayscale format, each pixel contained a value ranging from 0 to 255 based on the intensity captured by the 8-bit camera sensor. In the next step, the intensity values were mapped to the new values such that 1% of data were saturated at low and high intensities of the image. This made possible to increase the contrast of the output image. To identify the background of an image a morphological closing operation was used, which dilated and eroded the image consecutively using a structuring element of a disk shape with a radius of 11 pixels. In the next step, the background was subtracted from the contrasted image, which is then followed by binarisation using Otsu's method. The image included a near nozzle flat sheet region and a downstream atomised region. The flat sheet region was filtered out from the image by selecting the longest network of interconnected pixels in the binarised image. The discontinuities in the sheet structure were then conjoined using the same closing operation as the one used for background detection, however in this case we use a structural element of 2 pixels in radius. After identifying and filling the sheet structure, a combination of addition and subtraction to the binarised image were used to obtain the downstream atomised region. The sheet structure was used to derive information such as breakup length, width and spray angle, while the downstream atomised region was analysed to reconstruct the particle (hereafter, droplets are referred to as particles) distribution. A typical decomposition using in the analysis is presented in Fig. 2.
To study the particle distribution, a 20 $\times$ 20 grid was used dividing the image into 400 grid elements of 0.8 $\times$ 1.024 mm^2 in size. All the particle locations and their respective properties were identified within each grid element across all consecutive time frames. Overall, approx. 1 million particles were identified in the batch of 2000 images, with over 10,000 per grid element in the denser areas. Properties such as number density, polydispersity and Sauter mean diameter were calculated and analysed across all grid elements which are required for comparison with the FLA modelling data. The equivalent particle diameter is calculated based on the projected surface area of the particles, where $d_{eq} = \sqrt{4A/\pi}$. The error in measurement for this parameter is of the order of a pixel size which is 20 μm.

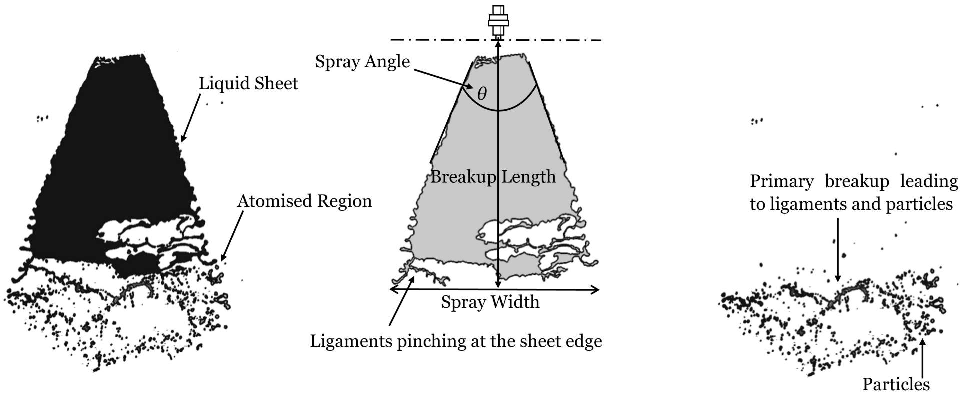

Figure 2. Schematic depicting the process followed to analyse flat fan sprays.

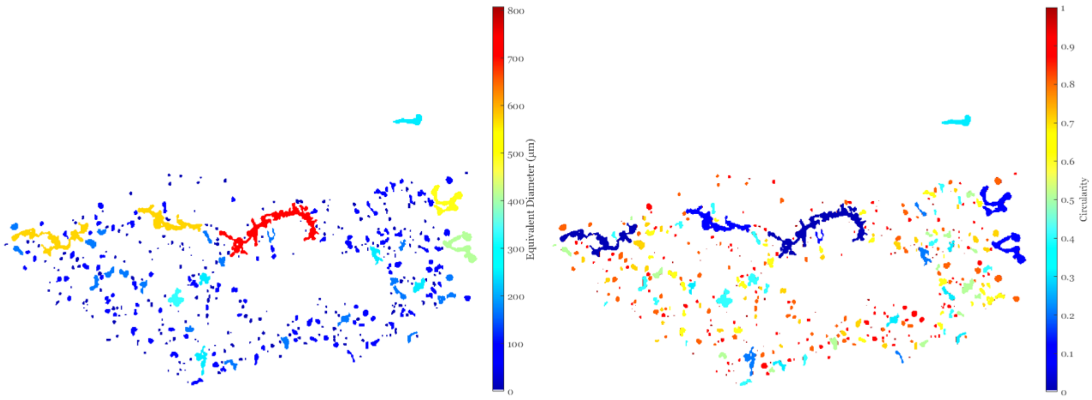

Figure 3. Liquid structures in the atomised region coloured by their equivalent diameter (left) and circularity (right).

Results and Discussion

Some results of the analysis conducted using the image processing algorithms described in the previous section are presented in Figs. 3 and Fig. 4. Here our analysis is focussed on identification of structures in the spray. A typical picture of such structures is presented in Fig. 3. In this figure, the structures are coloured to denote their equivalent diameter (Fig. 3, left) and circularity (Fig. 3, right). There is a correlation between the two parameters, the larger the structures, the smaller is the corresponding circularity (for circles, the circularity is 1).

In the upper atomised region nearer to the liquid sheet, there are more large ligaments, which break down into smaller particles downstream. In Fig. 4, left, the average values of the Sauter mean diameter, which is representative of the overall size of these particles in each grid element, are presented. D_{32} values are higher in the region were the spray transforms from sheet into stretched ligaments and particles and along the edges of the spray. Fig.4, middle, shows the variance of D_{32}, it can be interpreted to indicate the level of polydispersity in particle size distribution. The top and regions along the edges of the spray have higher degree of polydispersity. Finally, it important to note the choice of the criteria distinguishing between ligaments and particles. This criteria was used in filtering of data, when calculating the Sauter mean diameter, i.e. only the particles, which meet the criteria, are included in the calculation of the Sauter mean diameter. Figs. 4 left and right show average D_{32} distribution obtained for two different threshold values of circularity 0.3 and 0.5. As it can be seen from these two figures, the results depend on the selected criteria.

Conclusions

An image processing algorithm to analyse particle distribution in flat fan sprays has been developed, it is based on identification of structures in spray and collecting statistics about the structures across all time frames. The algorithm can map spray characterisation parameters

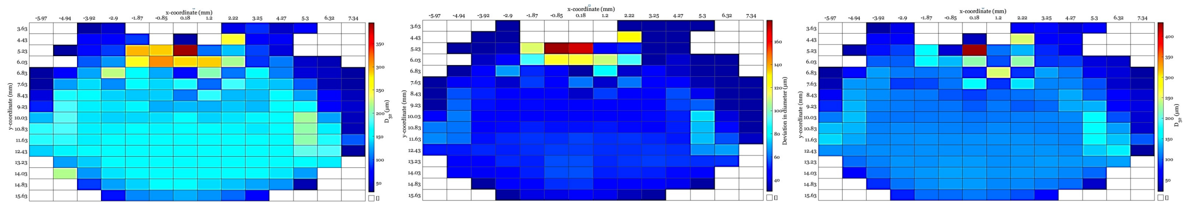

Figure 4. Average Sauter mean diameter across the field (left) assuming critical circularity is 0.3, and corresponding deviation (middle); average Sauter mean diameter across the field assuming critical circularity is 0.5 (right).

such as Sauter mean diameter, level of polydispersity, and number density. It's been identified that the selection of the criteria in identification of structures is important as the outputs are sensitive to the threshold. It is proposed to extend the criterion to include velocities as well as the geometry of the structures.

Acknowledgements

The work is supported by the University of Brighton (PhD Studentship) and the UKRI (Grant MR/T043326/1). The authors are grateful to Dr Guillaume De Sercey and Prof Cyril Crua for help and advice.

Nomenclature

D_{32}	Sauter mean diameter, volume-surface mean diameter
FLA	fully Lagrangian approach also known as Osiptsov's method [3]

References

[1] Sazhin, S. S., 2014, "Droplets and Sprays". Springer.
[2] Begg, S., Kaplanski, F. B., Sazhin, S. S., Hindle, M., and Heikal, M., 2009, *International Journal of Engine Research*, 10 (4), pp. 195-214.
[3] Osiptsov, A. N., 2000, *Astrophysics and Space Science*, 274 (1-2), pp. 377-386.
[4] Healy, D. P., and Young, J. B., 2005, *Proceedings of the Royal Society of London A: Mathematical, Physical and Engineering Sciences*, 461 (2059), pp. 2197-2225.
[5] Li, Y., Rybdylova, O., 2021, *International Journal of Multiphase Flow* 142, 103716.